

High-pressure study of ScH₃: Raman, infrared, and visible absorption spectroscopy

Tetsuji Kume*

Department of Materials Science and Technology, Faculty of Engineering, Gifu University, 1-1 Yanagido, Gifu 501-1193, Japan

Hiroyuki Ohura and Tomoo Takeichi

Environmental and Renewable Energy Systems, Graduate School of Engineering, Gifu University, 1-1 Yanagido, Gifu 501-1193, Japan

Ayako Ohmura

Center for Transdisciplinary Research, Niigata University, 8050 Ikarashi Ni-no-cho, Niigata 950-2181, Japan

Akihiko Machida, Tetsu Watanuki, and Katsutoshi Aoki

Quantum Beam Science Directorate, Japan Atomic Energy Agency, Hyogo 679-5148, Japan

Shigeo Sasaki and Hiroyasu Shimizu

*Department of Materials Science and Technology, Faculty of Engineering, Gifu University, 1-1 Yanagido, Gifu 501-1193, Japan and
Environmental and Renewable Energy Systems, Graduate School of Engineering, Gifu University, 1-1 Yanagido, Gifu 501-1193, Japan*

Kenichi Takemura

Advanced Nano Materials Laboratory, National Institute for Materials Science (NIMS), Tsukuba 305-0044, Japan

(Received 11 March 2011; revised manuscript received 14 June 2011; published 31 August 2011)

Raman, IR, and visible absorption spectra of scandium trihydride (ScH₃) have been measured at high pressures up to 50 GPa, to investigate the structural and electronic phase transitions. Successive hcp-intermediate-fcc phase transitions were observed at 25 and 46 GPa by Raman and IR measurements. It was suggested that the intermediate phase of ScH₃ takes the same structure as that of YH₃ with a long periodicity of the stacking of the metal planes. The visible absorption spectra allowed us to determine that the energy gap of ScH₃ is 1.7 eV at the ambient condition and is closed around 50 GPa, at which the crystal structure transforms to fcc.

DOI: 10.1103/PhysRevB.84.064132

PACS number(s): 61.50.Ks, 71.30.+h, 71.20.Eh, 78.30.Hv

I. INTRODUCTION

Rare-earth metal hydrides (RH_x) have long attracted attention as interesting systems that show both structural and electronic (metal-insulator) phase transitions driven by the inclusion of hydrogen (hydrogenation). Yttrium (Y) and lanthanum (La) have been the most extensively investigated metal hydrides.^{1–12} Metal YH₂ with an fcc structure transforms to insulator YH₃ with a hexagonal structure, in which the Y lattice crystallizes into the hcp structure and accommodates H atoms into tetrahedron (T) and octahedron (O) sites. The H atoms in the O site are known to be positioned not at the center of the octahedron but near the metal basal planes. For La with an ionic radius larger than that of Y, a structural transition does not occur, but a metal-insulator transition does occur during hydrogenation from LaH₂ to LaH₃.

RH₃ with an hcp structure such as YH₃ undergo a pressure-induced transition to the fcc structure. Palasyuk and Tkacz^{13–17} reported the systematic change in the transition pressure for RH₃ (R = Sm, Gd, Ho, Er, Lu, and Y); they found that the phase transition pressure linearly increases as the atomic number of the rare-earth metal decreases. Recently, high-pressure synchrotron XRD experiments on YH₃ by Machida *et al.*^{18,19} revealed an intermediate phase in between the hcp and fcc phases. The intermediate phase was suggested to have a structure with a long periodicity of a stacking of yttrium. Kume *et al.*²⁰ reported the intermediate phase characteristics of the Raman spectra, and they proposed the following mechanism for the phase transition from the hcp to the intermediate phase:

displacement of the H atoms in the O site from the metal plane toward the center of the octahedron triggers the sliding of the metal basal planes (the *c* planes), resulting in the phase transition.

In addition to the pressure-induced structural change, the pressure-induced electronic change has also attracted attention. According to high-pressure optical studies of YH₃,^{20,21} band-gap closure was suggested to occur at 25 GPa for the fcc phase. Dense metal YH₃ has received an increasing attention because of its high-*T_c* superconductivity, which was recently predicted by Kim *et al.*²² More recently, a theoretical investigation of YH₃ has predicted the existence of an intermediate phase and has realized its insulating property by a Peierls distortion.²³

Scandium (Sc) is the lightest element with the smallest ionic radius among the rare-earth metals. The crystal structure and electronic properties of ScH₃ have not been well investigated because a high hydrogen gas pressure is needed to obtain ScH₃ and ScH₃ reversibly decomposes into ScH₂ and H₂ upon releasing the hydrogen pressure. ScH₃'s detailed structure, including the hydrogen positions, has been recently determined by neutron diffraction experiments.²⁴ Substoichiometric ScH_{2.9} is shown to have a crystal structure with *P6₃mmc* symmetry. The octahedron sites (O sites) for hydrogen atoms are split into two sites positioned near the metal basal plane. The O site hydrogen atoms randomly occupy one of the two equivalent positions, in contrast to YH₃ in which the hydrogen atoms are ordered.^{9,10}

Recently, the pressure-induced structural phase transition in ScH_3 has been investigated by synchrotron XRD experiments using a diamond anvil cell (DAC).²⁵ These experiments suggested that ScH_3 undergoes the phase transition from the hcp to the fcc structure via an intermediate state in the pressure region between 30 and 46 GPa. This implies that the hcp-intermediate-fcc structural change is the common transition sequence of RH_3 under high pressure. However, the detailed structure of the intermediate phase of ScH_3 has not been resolved. Not only the structural change but also gap closure (metallization) under high pressure are interesting topics of study, because YH_3 (and therefore ScH_3) may be a high- T_c superconductor.²² However, there has been no report on the pressure-induced insulator-metal transition in ScH_3 .

In this study, to investigate the pressure-induced structural and insulator-metal transformations in ScH_3 , we performed Raman scattering, IR, and visible absorption spectroscopies at room temperature at pressures up to 50 GPa. Raman and IR signals related to Sc and H vibrations were clearly observed up to ~ 40 GPa and were found to change in correspondence to the hcp-intermediate and intermediate-fcc phase transitions. The Raman spectra of ScH_3 and YH_3 intermediate phases strongly suggested that the intermediate phase of ScH_3 has the same structure as that of the intermediate phase of YH_3 . Visible absorption measurements demonstrated that the optical gap energy estimated under the assumption of an indirect gap decreases from 1.7 eV at 1 atm (0 GPa) to 0 eV at ~ 50 GPa. Gap closure is predicted to be complete just after the transition to the fcc phase.

II. EXPERIMENTAL

We used a DAC to synthesize the ScH_3 by hydrogenating an Sc foil and to carry out high-pressure experiments. A small piece of Sc (nominal purity 99.9%) was pressed between the diamond anvils to obtain the thin foil. Then the Sc foil was placed in a sample chamber, which was made by drilling a hole in a preindented tungsten (W) gasket of about 0.03-mm thickness. The sample chamber containing the Sc foil was filled with gaseous hydrogen compressed to 180 MPa using a gas loading system.²⁶ To avoid the inclusion of the contaminants, the gas-loading system was evacuated. Sc was hydrogenated, and the remaining hydrogen around the sample functioned as the pressure medium. Pressure was calibrated by the ruby fluorescence method with the quasihydrostatic ruby scale.²⁷

Raman spectra were measured at room temperature in backscattering geometry with a triple polychromator (JASCO NR 1800) equipped with a charge-coupled device detector. A solid-state laser (Coherent Verdi2W) provided incident 532-nm radiation with a power of 5 mW. The measured Raman spectra contained the signals from H_2 . Therefore, we extracted the spectra of ScH_3 by subtracting the H_2 spectrum multiplied by an appropriate factor so as to cancel out the H_2 signals. The thickness of the sample for the Raman measurements was approximately 2–3 microns.

To obtain the optical band gap energy, visible absorption experiments were carried out using an apparatus equipped with a pair of Cassegrain focusing mirrors, a single monochromator, and a multichannel detector.²⁸ A very thin foil of approximately 1–2 microns thick was prepared as the sample for

transmission measurements. The visible absorption spectra were obtained from $-\ln(I/I_0)$, where I and I_0 were the transmitted light intensities of the sample and the reference, respectively. The reference signals were measured by focusing the light on an area in which the sample was absent.

We also investigated the IR active vibrations of ScH_3 by reflectivity measurements. Although transmission measurements are often adopted, it is difficult to measure the reference signal under high pressures, because the sample chamber shrinks; therefore, reflectivity measurements are preferable for our case. The reflectivity measurements were performed with the aid of a microscopic FTIR spectrometer.²¹ By using the light intensity reflected from the metal W gasket as a reference signal (R_w), the reflectivity spectra of the sample were obtained as R_s/R_w . The IR active lattice vibrations give rise to anomalies in not only the imaginary part of the refractive index (absorption coefficient) but also the real part, which leads to the peaks in the IR reflectivity spectra.

Previous high-pressure XRD experiments²⁵ indicated that the sample at low hydrogen pressures below 5 GPa is a mixture of hexagonal ScH_3 , fcc ScH_2 , and hexagonal ScH_x with $x \sim 0.43$. As the pressure increased up to 5.3 GPa, ScH_x changed to ScH_2 and ScH_3 . The volume fraction of ScH_2 was 68% at 5.3 GPa and 25% at 20.9 GPa. Even at 46 GPa, XRD peaks from fcc ScH_2 were observed. This was true for a previous study with a 15-micron-thick sample.²⁵ Since the current study used a sample that was at most 5 microns thick, the volume fraction of ScH_2 is believed to be much less than that in the previous sample.

III. RESULTS AND DISCUSSION

A. Raman and IR reflection spectra of hcp ScH_3

Figure 1 shows the IR reflectivity spectra measured at pressures below 8 GPa. As the pressure increased, reflectivity generally decreased, indicating the formation of transparent ScH_3 .

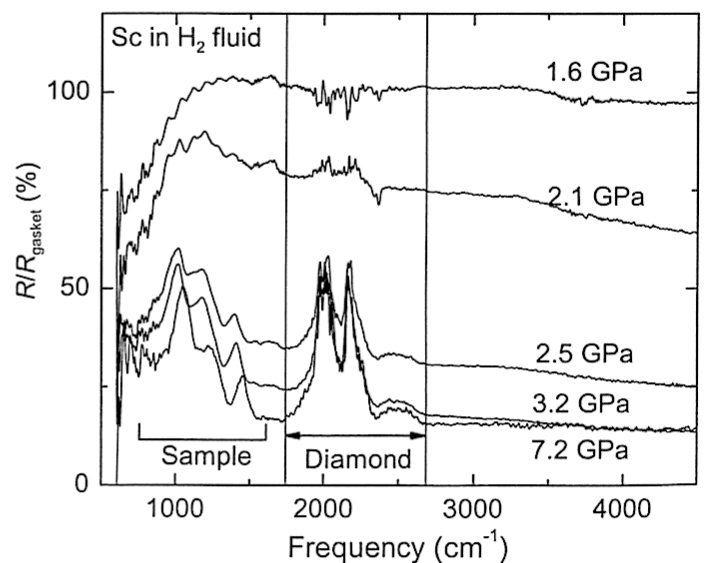


FIG. 1. Pressure dependence of reflectivity spectra in IR region. The decrease in the reflectivity corresponds to progress of hydrogenation. Signals in the region of 1750–2700 cm^{-1} are due to the diamond anvils.

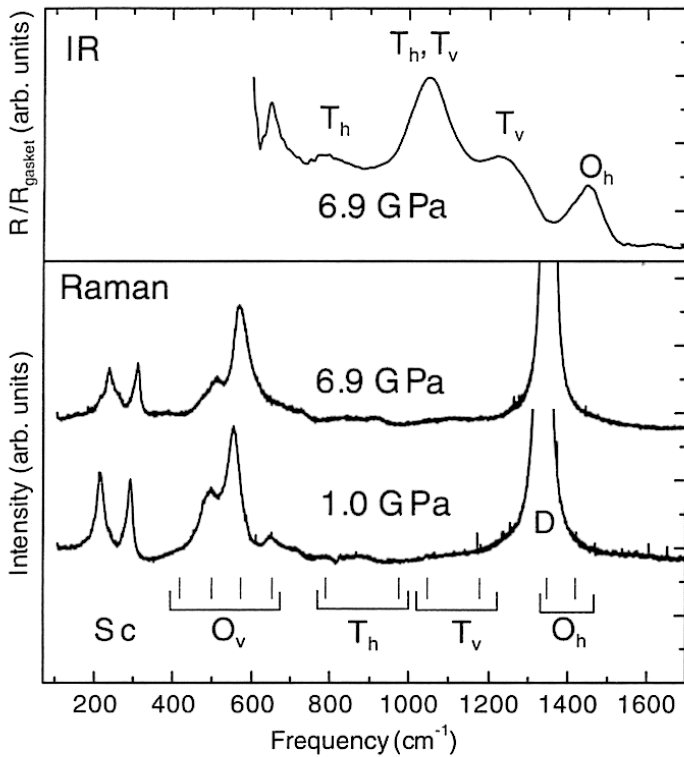


FIG. 2. Typical IR and Raman spectra of ScH_x obtained in the low-pressure region. The ticks correspond to the peak positions of experimental phonon density states of $\text{ScH}_{2.9}$ (Ref. 24). O_v (O_h) indicates that hydrogen at the octahedron site vibrates vertically (horizontally) to the c plane, and O_v (T_h) indicates that H at the tetrahedron site vibrates vertically (horizontally) to the c plane. The peaks denoted by Sc are attributed to vibrations of the Sc lattice. The strong signals denoted by D are due to the diamond anvils.

The well-hydrogenated sample (≥ 2.5 GPa) showed peaks in the $600\text{--}1700\text{ cm}^{-1}$ range. The peak positions are consistent with those of the phonon density of state measured by neutron experiments on $\text{ScH}_{2.9}$.²⁴ Even in the well-hydrogenated sample, a small amount of fcc ScH_2 exists; however, the IR signals from fcc ScH_2 are negligible because its metallic nature allows only shallow penetration of IR light. Therefore, these peaks are regarded as vibrational signals from ScH_3 .

Figure 2 shows typical Raman and IR reflection spectra measured at low pressures (≤ 10 GPa). All the present Raman signals are considered to be caused by hcp ScH_3 for the following reasons. Even if fcc ScH_2 exists in our sample, the signals of ScH_2 signals are not observed because only one weak peak is predicted to appear around 1200 cm^{-1} close to the very strong diamond signal (1330 cm^{-1}). Furthermore, two strong peaks from Sc lattice vibrations were found at frequencies below 300 cm^{-1} ; by analogy with YH_3 ,^{7,8} the higher- and lower-frequency bands were assigned to a breathing and a shear mode of Sc, respectively. In addition, H-related bands were assigned by following previous assignments for phonon density of state (PDOS) peaks obtained by neutron inelastic scattering.²⁴ In Fig. 2, the positions of PDOS peaks are indicated with bars; O_v (T_h) indicates, for example, that the hydrogen at the octahedron (tetrahedron) site vibrates vertically (horizontally) to the c plane. The PDOS peaks do not always correspond to Raman or IR peaks. Since, however,

the phonon dispersion curves of hydrogen in the rare-earth hydrides show flat features,¹⁰ indicating that the PDOS peak positions are in good agreement with those of the Raman and IR spectra.

In Fig. 2, strong Raman-active O_v modes are observed. This is compatible with the fact that the H atoms of the O site (H_O) are not located at the center of the octahedron.²⁴ If the H atoms are centered in the O site, the H vibrations become Raman inactive.

B. Pressure dependence of vibrational spectra

Figure 3 shows Raman spectra of ScH_3 for different pressure. Changes in the Raman spectral shape correspond to the structural phase transitions at 25 and 40 GPa, which have been reported in results from previous XRD measurements.²⁵ The former and latter are the hcp-intermediate and intermediate-fcc phase transitions, respectively. Figure 3 shows that the phase transition from the hcp to the intermediate phases at 25 GPa results in characteristic changes in the Raman spectrum; the lowest Sc vibrational peak discontinuously shifts to lower frequencies and the O_v peaks almost disappear. These spectral changes are analogous to those observed in a previous Raman study of YH_3 .²⁰ Following the results of this previous study,²⁰ the discontinuous shift of the Sc mode is explained by the change in the stacking sequence of metal Sc layers, and the disappearance of the O_v mode is explained by the centering

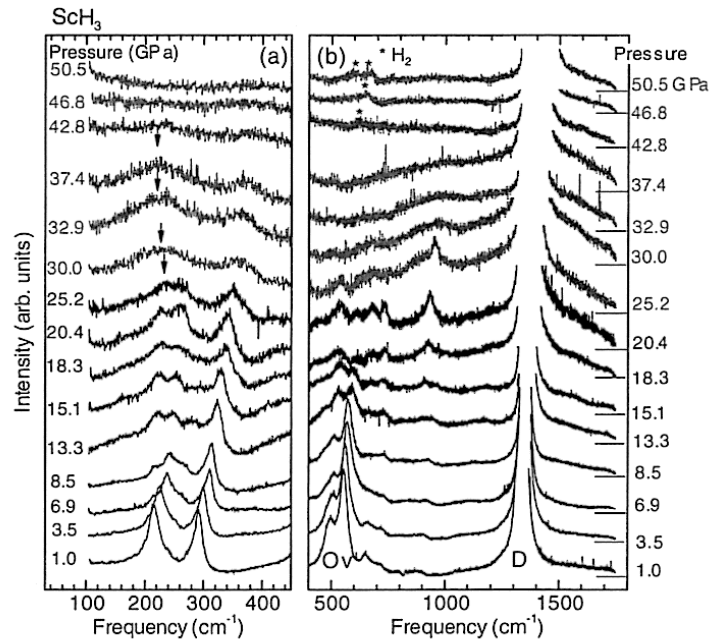


FIG. 3. (Color online) Pressure dependence of Raman spectra of ScH_3 . (a) and (b) correspond to the low-frequency ($0\text{--}450\text{ cm}^{-1}$) and high-frequency ($400\text{--}1750\text{ cm}^{-1}$) regions, respectively. Horizontal bars in (b) indicate the vertical offset of each spectrum. The spectral characteristics of the hexagonal, intermediate, and fcc phases were observed at $P < 25$ GPa, $25\text{ GPa} < P < 43$ GPa, and $43\text{ GPa} < P$, respectively. O_v indicates that the signals around 500 cm^{-1} correspond to the signals from hydrogen at the octahedron site that vibrates vertically to the c plane. D indicates that the strong signals around 1330 cm^{-1} correspond to the signals from diamond anvils. Asterisks correspond to signals from the hydrogen pressure medium.

TABLE I. Vibrational irreducible representations of fcc ScH_3 with $Fm\bar{3}m$. “R” or “ir” in parentheses correspond to the Raman and IR active modes, respectively.

Atom	Site symmetry	Irreducible representation
Sc	4a	$T_{1u}(\text{ir})$
H in O site	4b	$T_{1u}(\text{ir})$
H in T site	8c	$T_{2g}(\text{R}) + T_{1u}(\text{ir})$

of H_2O . Above 45 GPa, all the Raman peaks disappear due to the transition to the fcc phase. Table I presents the vibrational modes of fcc ScH_3 analyzed on the basis of group theory. Note that fcc ScH_3 shows only one Raman-active vibration of H in the T site (H_T). Its frequency is estimated to be $\sim 1200 \text{ cm}^{-1}$ by considering the H_T mode frequency of fcc YH_2 (1142 cm^{-1}) at the ambient condition and the pressure-induced shift. However, the H_T mode is not detected because of the strong diamond signal around 1330 cm^{-1} .

Figure 4 shows the IR reflectivity spectra measured at various pressures. The H-related vibrational peaks were detected at pressures up to 34 GPa. Note that all the peaks observed here shift to higher frequencies with increasing pressure. In addition, the following spectral changes occur at the hcp-intermediate phase transition at 28 GPa: (1) the fine structures of 3 \sim 4 small O_v peaks at $\sim 800 \text{ cm}^{-1}$ become a strong band, (2) at 1200 cm^{-1} , a small shoulder appears in the peak on the lower frequency side, and (3) the peak

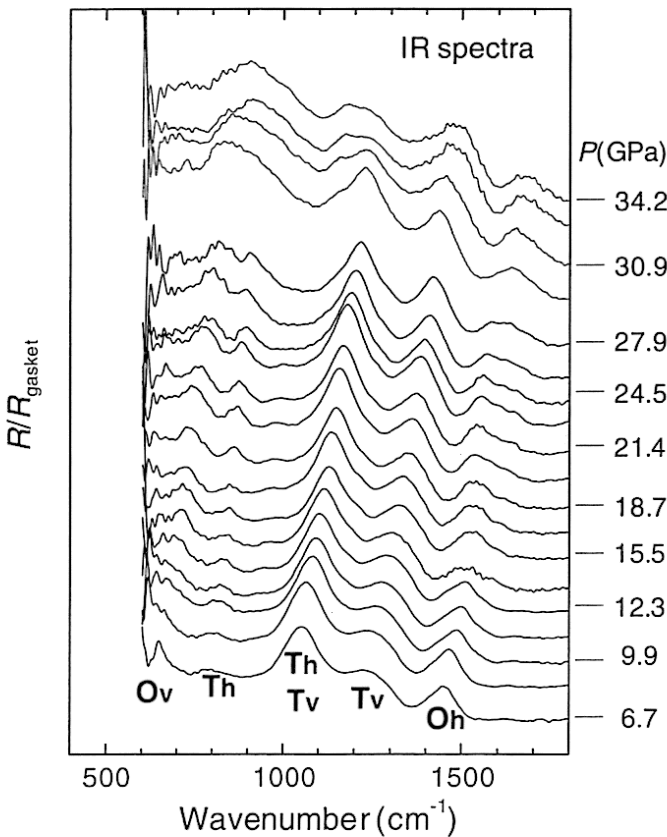


FIG. 4. (Color online) Pressure dependence of IR reflection spectra of ScH_3 . O_v , O_h , T_v , and T_h are the same as described in the legend of in Fig. 2.

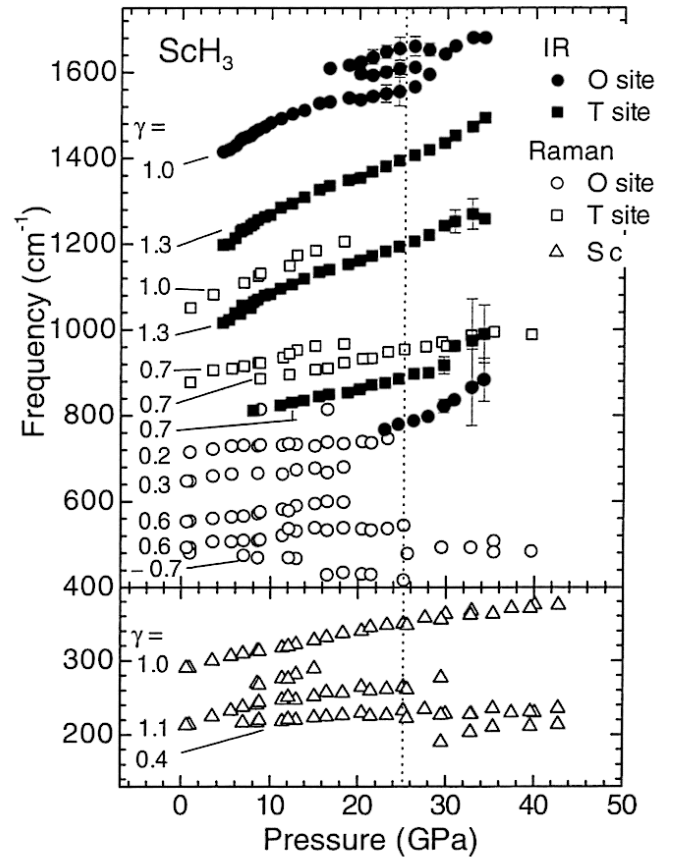


FIG. 5. Pressure dependence of the vibrational frequencies of ScH_3 obtained upon compression. Solid and open symbols correspond to IR and Raman data, respectively. Circles, squares, and triangles indicate vibrational signals from H in the O site, H in the T site, and Sc, respectively. The values of the mode Grüneisen parameters γ in the hexagonal phase are shown. Error bars represent the peak width of the signals. The dashed line corresponds to transformation from the hexagonal to the intermediate phase.

shape of the O_h mode at $\sim 1600 \text{ cm}^{-1}$ changes. The O_v peak at 800 cm^{-1} increases in intensity in the intermediate phase, in contrast to the Raman-active O_v peaks (Fig. 3), which disappear upon transitioning to the intermediate phase. This arises from the compensative selection rules between the Raman and IR absorptions.

We note here that the hcp-intermediate phase transition was identified by the IR measurements at 28 GPa, the Raman measurements at 25 GPa, and the XRD measurements at 30 GPa.²⁵ This dispersion can be explained by the fact that the phase transition is of the first order and the hcp and intermediate phases coexist at pressures between 25 and 30 GPa. The coexisting state has been reported for YH_3 .²⁰ For the present case, the lowest value (25 GPa) is plausible for the hcp-intermediate phase transition of ScH_3 . In contrast, for the transition from the intermediate to the fcc phase, the pressure determined by Raman experiments agrees well with that determined by XRD experiments ($P = 46 \text{ GPa}$).²⁵

Figure 5 shows the pressure dependence of the vibrational frequencies of ScH_3 obtained from the present Raman and IR experiments. Almost all the modes show a high-frequency shift, except for a Raman-active O_v mode at 480 cm^{-1} at 1 atm. We calculated the mode Grüneisen parameters (γ) given

in this figure as $\gamma = -d[\ln(\omega)]/d[\ln(V)]$ by using the volume (V) data.²⁵ The values of γ are in the range of 0.2 – 1.0 for the hydrogen modes at the O site apart from the softening mode (–0.7), while they are in the range of 0.7 – 1.3 for hydrogen mode at the T site. The value of the γ for the H vibration at the O site tends to be smaller than that at the T site, similar to the case of YH_3 .²⁰ A previous theoretical study²⁹ reported that the bonding nature between the hydrogen and metal atoms in rare-earth trihydrides is covalent for the O site but ionic for the T site. The difference in the bonding nature is considered to be responsible for the difference between the values of γ for the O and T sites.

C. Intermediate phase

We now discuss the intermediate phase and its Raman and IR spectra shown in Fig. 6. A previous high-pressure synchrotron XRD study of YH_3 resolved the structure of the intermediate phase as a long-period polytype with periodic arrangements of hcp-type and fcc-type stacking layers of Y metals. As shown in Fig. 6, the ScH_3 and YH_3 Raman spectra are similar as follows: both show two main peaks (denoted by solid circles) in the metal lattice modes. These spectral similarities arise from the structural similarities of the Sc and Y metal lattices. Spectral similarities also exist in the hydrogen vibrations; the O_v modes disappear in the intermediate phase and an

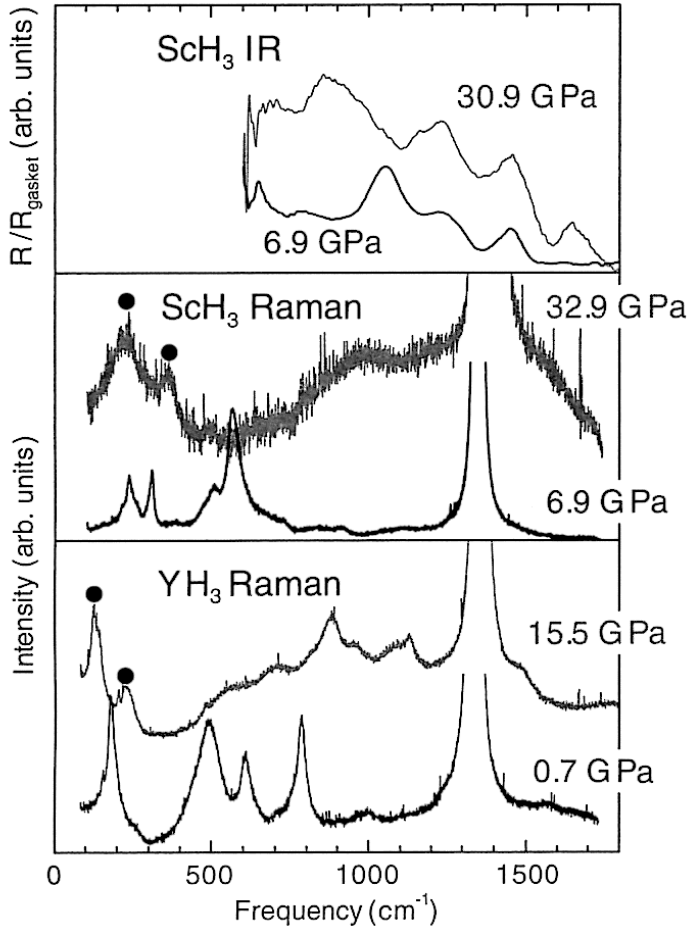


FIG. 6. (Color online) IR and Raman spectra measured in the hcp (black) and intermediate (blue) phases. For the Raman data, the previous YH_3 data are also shown for comparison. The Raman peaks denoted by solid circles are characteristic of the intermediate phase.

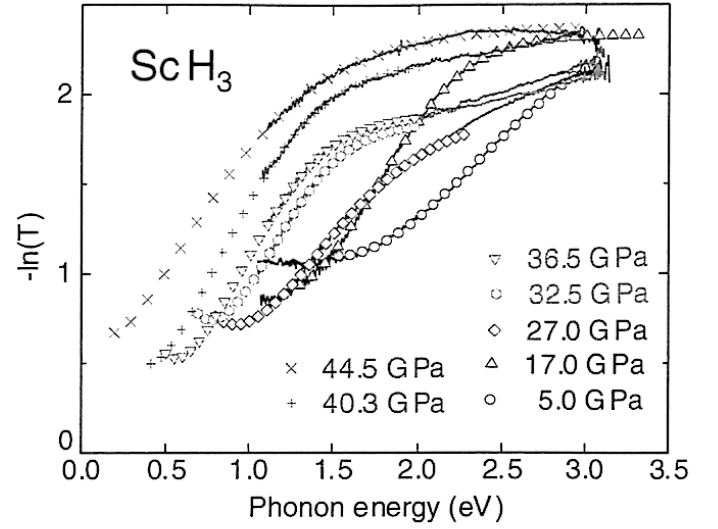


FIG. 7. (Color online) Pressure dependence of absorption spectra of ScH_3 . The measured and fitted spectra are shown by solid lines and symbols, respectively. For theoretical fitting, see text.

extremely broad Raman band ranging from 500 to 1700 cm^{-1} appears instead. A broad band is also observed in the IR spectrum (Fig. 6). Hence, the H position in the octahedron can be discussed using these spectral features. If the H atoms are centered in the octahedron, no Raman peak resulting from H in the O site is observed. Therefore, it is suggested that on the phase transition to the intermediate phase, the H in the O site shifts from the metal basal plane toward the center. However, the H atoms are not likely to be located at the center for every octahedron owing to the complex stacking of the layers. The extremely broad band possibly reflects positionally disordered hydrogen atoms around the center of the O site.

A recent theoretical paper on the high-pressure phase of YH_3 ²³ suggested that the intermediate phase is a periodically distorted form of the fcc structure. This distortion was identified as a Peierls distortion, which results in a vertical modulation (c direction) of H positions with a horizontally propagating wave vector. Furthermore, the occurrence of an energy gap due to the Peierls distortion was reproduced. In the theoretically reproduced intermediate phase, the amplitude of H modulation wave is larger in the O site than in the T site. That is, the positions of H atoms fluctuate spatially in each O site. These theoretical predictions are consistent with our interpretation of the vibrational spectra of YH_3 and ScH_3 intermediate phases. The extremely broad bands of the H modes suggest the positional disorder of H position, as mentioned above. The H disorder may correspond to the fact that the modulation wavelength is much larger than, or is not commensurately matched with, the lattice constants. The low-temperature Raman measurements will be crucially important for a more detailed discussion. Such experiments will be performed in the near future.

D. Pressure dependence of the optical gap of ScH_3

Figure 7 indicates the visible absorption spectra measured under various pressures. In this figure, the experimentally obtained spectra are indicated by solid lines. The absorption edge shifted to lower energies with increasing pressure. From the absorption edges, we attempted to obtain the band gap

energies by a theoretical fitting. According to a previous paper,⁶ the hcp phase of YH₃ has been interpreted as an indirect gap insulator. Although an appropriate scheme for optical absorption in ScH₃ has not been well established, we assumed an indirect allowed transition for ScH₃ by considering the structural similarity to YH₃. In the case of the indirect allowed transition, the absorption coefficients α near the band gap energy E_g is written as

$$\alpha(\omega) = A \frac{(\hbar\omega - E_g)^2}{\hbar\omega}. \quad (1)$$

For actual analysis, opaque metallic ScH₂ should be included and a sample size smaller than the illuminated spot of the incident light should be considered. The existence of ScH₂ increases the background signals because metallic ScH₂ has a large extinction coefficient. The extinction coefficient of ScH₂ is expected to be independent of the incident photon energy throughout the visible region. Hence, the presence of ScH₂ reduces the incident intensity I_0 by a factor C (≤ 1). Thus, the transmitted light intensity I should be expressed as,

$$I = CI_0(1 - R)^2 \exp(-\alpha d), \quad (2)$$

where R and d correspond to the reflectivity and thickness of the sample, respectively. Because the sample is small compared with the illuminated spot, part of the incident light is not transmitted through the sample. Therefore, I should be rewritten as,

$$I = tCI_0(1 - R)^2 \exp(-\alpha d) + (1 - t)I_0, \quad (3)$$

where t is the ratio of the total area illuminated on the sample to the spot size of the incident light. Because the absorption spectrum is $-\ln(I/I_0)$, we thus fitted the experimental absorption spectra using the function

$$-\ln(I/I_0) = -\ln[C_1 \exp(-\alpha d) + C_2]. \quad (4)$$

The fitted absorption curves are shown by open symbols in Fig. 7. We find that the calculated absorption edge reproduces well the experimental one for all the spectra. The agreement of the fitted curve to the data is fairly good even for the intermediate phase ($P \geq 25$ GPa), although the appropriate optical transition scheme has not yet been established.

Figure 8 shows the pressure dependence of E_g obtained from fitting the data. For comparison, the results for YH₃ (Ref. 20) are also indicated. The energy gap of ScH₃ at 1 atm is extrapolated to 1.7 eV, which is lower than that of YH₃. With increasing pressure, E_g is gradually decreased. Gap closure (metallization) occurs at ~ 50 GPa.

As seen in Fig. 8, the insulator-metal transition occurred almost simultaneously with the structural change to the fcc phase ($P \sim 45$ GPa). In addition, metallization occurred simultaneously with structural change for YH₃.^{18,21} According to theoretical studies of YH₃,^{2,23} the insulating properties of the intermediate and hcp phases are attributed to wavelike H modulation and interpreted in terms of the gap opening due to the Peierls distortion. Thus, the relaxation of the distortion in the fcc structure is predicted to cause metallization. This theoretical prediction is compatible with experimental studies of YH₃ and ScH₃, indicating that gap closure and transition to the fcc phase occur simultaneously.

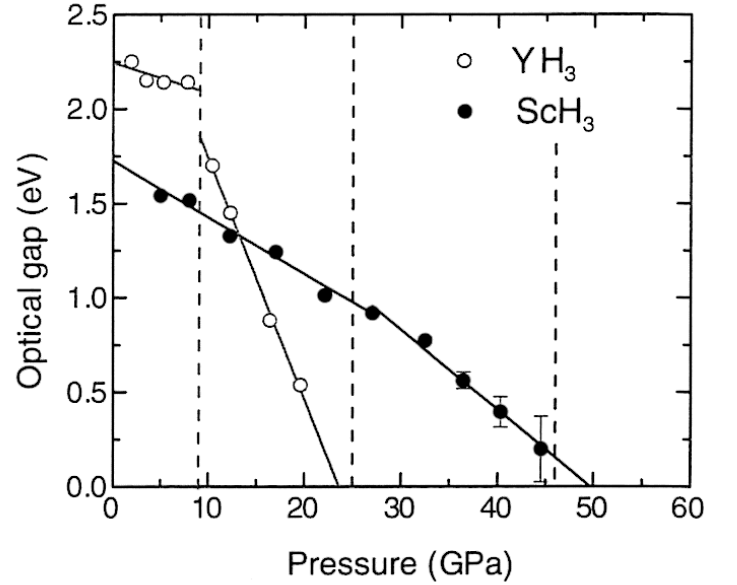


FIG. 8. (Color online) Pressure dependence of the optical gap energy of ScH₃. The optical energy gaps estimated by fitting the data (see text) are plotted. The previous data obtained for YH₃ are also plotted. Solid lines serve as guides to the eye. Dashed lines correspond to the structural phase transitions.

According to a recent theoretical study on the superconductivity of YH₃,²² T_c as high as 40 K was predicted to be achieved around 17 GPa in the fcc metallic phase. This high T_c originates from strong electron-phonon coupling resulting from the hybridization between the d state of Y and the s state of H in the O site. By analogy with the phonon spectral feature and the phase transition mechanism in YH₃, metallic fcc ScH₃ is also a candidate high- T_c superconductor. Because ScH₃ is lighter than YH₃, it should have a higher T_c . The experimental verification of a high T_c for YH₃ or ScH₃ will be one of the most interesting subjects in the field of metal hydrides.

IV. CONCLUSION

The structural-phase transitions and the insulator-to-metal transition for ScH₃ were investigated by means of Raman, IR, and visible absorption spectroscopies under high pressures. The evolution of the Raman and IR spectra was investigated through the hcp, intermediate, and fcc phases. The Raman spectra of the intermediate phase of ScH₃ were analogous to those of the intermediate phase of YH₃. This suggests that ScH₃ has a long-period polytype structure, similar to that reported for YH₃. Gap closure of ScH₃ investigated by visible absorption spectroscopy was estimated to occur around 50 GPa in the fcc phase. Based on the previous theoretical studies,^{2,23} the simultaneous occurrence of metallization and transition to fcc phase can be interpreted as the relaxation of the Peierls distortion.

ACKNOWLEDGMENTS

This study has been partially supported by New Energy and Industrial Technology Development Organization (NEDO) under Advanced Fundamental Research Project on Hydrogen Storage Materials.

*kume@gifu-u.ac.jp

- ¹J. N. Huiberts, R. Griessen, J. H. Rector, R. J. Wijngaarden, J. P. Dekker, D. G. de Groot, and N. J. Koeman, *Nature (London)* **380**, 231 (1996).
- ²Y. Wang and M. Y. Chou, *Phys. Rev. Lett.* **71**, 1226 (1993).
- ³T. J. Udovic, J. J. Rush, Q. Huang, and I. S. Anderson, *J. Alloys Compd.* **253-254**, 241 (1997).
- ⁴T. J. Udovic, Q. Huang, R. W. Erwin, B. Hjörvarsson, and R. C. C. Ward, *Phys. Rev. B* **61**, 12701 (2000).
- ⁵A. T. M. van Gogh, E. S. Kooij, and R. Griessen, *Phys. Rev. Lett.* **83**, 4614 (1999).
- ⁶A. T. M. van Gogh, D. G. Nagengast, E. S. Kooij, N. J. Koeman, J. H. Rector, R. Griessen, C. F. J. Flipse, and R. J. J. G. A. M. Smeets, *Phys. Rev. B* **63**, 195105 (2001).
- ⁷A.-M. Racu and J. Schoenes, *Phys. Rev. Lett.* **96**, 017401 (2006).
- ⁸J. Schoenes, A.-M. Racu, M. Rode, and S. Weber, *J. Alloys Compd.* **446-447**, 562 (2007).
- ⁹P. van Gelderen, P. J. Kelly, and G. Brocks, *Phys. Rev. B* **63**, 100301 (2001).
- ¹⁰P. van Gelderen, P. J. Kelly, and G. Brocks, *Phys. Rev. B* **68**, 094302 (2003).
- ¹¹J. A. Alford, M. Y. Chou, E. K. Chang, and S. G. Louie, *Phys. Rev. B* **67**, 125110 (2003).
- ¹²A.-M. Carsteanu, M. Rode, D. Zur, A. Borgschulte, H. Schröter, and J. Schoenes, *Phys. Rev. B* **69**, 134102 (2004).
- ¹³M. Tkacz and T. Palasyuk, *J. Alloys Compd.* **446-447**, 593 (2007).
- ¹⁴T. Palasyuk and M. Tkacz, *Solid State Commun.* **141**, 354 (2007).
- ¹⁵T. Palasyuk and M. Tkacz, *Solid State Commun.* **141**, 302 (2007).
- ¹⁶T. Palasyuk, M. Tkacz, and L. Dubrovinsky, *Solid State Commun.* **142**, 337 (2007).
- ¹⁷T. Palasyuk and M. Tkacz, *Solid State Commun.* **133**, 477 (2005).
- ¹⁸A. Machida, A. Ohmura, T. Watanuki, T. Ikeda, K. Aoki, S. Nakano, and K. Takemura, *Solid State Commun.* **138**, 436 (2006).
- ¹⁹A. Machida, A. Ohmura, T. Watanuki, K. Aoki, and K. Takemura, *Phys. Rev. B* **76**, 052101 (2007).
- ²⁰T. Kume, H. Ohura, S. Sasaki, H. Shimizu, A. Ohmura, A. Machida, T. Watanuki, K. Aoki, and K. Takemura, *Phys. Rev. B* **76**, 024107 (2007).
- ²¹A. Ohmura, A. Machida, T. Watanuki, K. Aoki, S. Nakano, and K. Takemura, *Phys. Rev. B* **73**, 104105 (2006).
- ²²D. Y. Kim, R. H. Scheicher, and R. Ahuja, *Phys. Rev. Lett.* **103**, 077002 (2009).
- ²³Y. Yao and D. D. Klug, *Phys. Rev. B* **81**, 140104(R) (2010).
- ²⁴V. E. Antonov, I. O. Bashkin, V. K. Fedotov, S. S. Khasanov, T. Hansen, A. S. Ivanov, A. I. Kolesnikov, and I. Natkaniec, *Phys. Rev. B* **73**, 054107 (2006).
- ²⁵A. Ohmura, A. Machida, T. Watanuki, K. Aoki, S. Nakano, and K. Takemura, *J. Alloys Compd.* **446**, 598 (2007).
- ²⁶K. Takemura, P. Ch. Sahu, Y. Kunii, and Y. Toma, *Rev. Sci. Instrum.* **72**, 3873 (2001).
- ²⁷R. J. Hemley, C. S. Zha, A. P. Jephcoat, H. K. Mao, L. W. Finger, and D. E. Cox, *Phys. Rev. B* **39**, 11820 (1989).
- ²⁸T. Kume, Y. Fukaya, S. Sasaki, and H. Shimizu, *Rev. Sci. Instrum.* **73**, 2355 (2002).
- ²⁹A. Fujimori, F. Minami, and N. Tsuda, *Phys. Rev. B* **22**, 3573 (1980).